Development 122, 1165-1174 (1996)
Printed in Great Britain © The Company of Biologists Limited 1996
DEV9438



# Widespread programmed cell death in proliferative and postmitotic regions of the fetal cerebral cortex

**Anne J. Blaschke[1], Kristina Staley and Jerold Chun[2,*]**

[1]Biology Graduate Program and [2]Neurosciences and Biomedical Sciences Graduate Program, The Department of Pharmacology, School of Medicine, University of California, San Diego, 9500 Gilman Drive, La Jolla, CA 92093-0636, USA

*Author for correspondence

## SUMMARY

**A key event in the development of the mammalian cerebral cortex is the generation of neuronal populations during embryonic life. Previous studies have revealed many details of cortical neuron development including cell birthdates, migration patterns and lineage relationships. Programmed cell death is a potentially important mechanism that could alter the numbers and types of developing cortical cells during these early embryonic phases. While programmed cell death has been documented in other parts of the embryonic central nervous system, its operation has not been previously reported in the embryonic cortex because of the lack of cell death markers and the difficulty in following the entire population of cortical cells. Here, we have investigated the spatial and temporal distribution of dying cells in the embryonic cortex using an in situ end-labelling technique called 'ISEL+' that identifies fragmented nuclear DNA in dying cells with increased sensitivity. The period encompassing murine cerebral cortical neurogenesis was examined, from embryonic days 10 through 18. Dying cells were rare at embryonic day 10, but by embryonic day 14, 70% of cortical cells were found to be dying. This number declined to 50% by embryonic day 18, and few dying cells were observed in the adult cerebral cortex. Surprisingly, while dying cells were observed throughout the cerebral cortical wall, the majority were found within zones of cell proliferation rather than in regions of postmitotic neurons. These observations suggest that multiple mechanisms may regulate programmed cell death in the developing cortex. Moreover, embryonic cell death could be an important factor enabling the selection of appropriate cortical cells before they complete their differentiation in postnatal life.**

Key words: programmed cell death, cerebral cortex, embryonic development, mouse

## INTRODUCTION

A requisite step in the development of the cerebral cortex is the generation and differentiation of its neurons. This begins with the 'birth' of neurons within proliferative zones adjacent to the ventricles (e.g. the ventricular zone or vz), and migration of these neurons to a superficial location consisting of postmitotic cells (e.g. the cortical plate or cp; see Boulder Committee, 1970). The extensive literature on embryonic cortical development that dates back decades (reviewed by Bayer and Altman, 1991) has been complemented more recently by analyses using retroviruses containing reporter genes (e.g. Walsh and Cepko, 1988; Price and Thurlow, 1988; Luskin et al., 1988; Austin and Cepko, 1990); these studies have enhanced our view of development to include details on the size, cell types and distribution of cortical clones.

In many of these studies, an implicit or explicit assumption has been that programmed cell death (PCD; Hamburger and Levi-Montalcini, 1949; Wyllie, 1981; Williams and Smith, 1993), if present at all, has a minor role during embryonic cortical development. However, PCD has been shown to play an important role in other embryonic systems (Saunders, 1966). In the chick, PCD has been observed in other parts of the embryonic CNS (Hamburger and Levi-Montalcini, 1949; Landmesser and Pilar, 1974; Hamburger, 1975; Clarke et al., 1976), where it is believed to participate in the formation of appropriate connections by matching neurons with their targets (Cowan et al., 1984; Raff et al., 1993). Since initial cortical connections are made during embryonic life (Rakic, 1976, 1977; Shatz and Rakic, 1981; Shatz et al., 1988), it is possible that PCD operates in the cortex during this period. Consistent with this hypothesis, PCD has been documented in the postnatal cerebral cortex (Heumann and Leuba, 1983; Finlay and Slattery, 1983; Price and Blakemore, 1985; Chun and Shatz, 1989; Ferrer et al., 1992), which may prove to be an extension of cell death processes occurring in the embryo.

A difficulty in investigating the prevalence and distribution of dying cells in situ has been the absence of specific cell death markers. Towards remedying this situation, several conceptually similar techniques, collectively termed 'in situ end-labelling' or ISEL, have been developed and used to examine PCD in other systems (Gavrieli et al., 1992; Wijsman et al., 1993; Wood et al., 1993). With these techniques, the double-

strand DNA breaks produced during PCD are identified by attaching labelled nucleotides to free DNA ends. The label can then be visualized in tissue sections, thus identifying dying cells by virtue of their nuclear DNA fragmentation. In every system thus far reported, ISEL has been shown to identify specifically cells undergoing PCD (Gavrieli et al., 1992; Wood et al., 1993; Wijsman et al., 1993; Homma et al., 1994; Surh and Sprent, 1994), including CNS cells in *Drosophila* (Abrams et al., 1993; White et al., 1994).

Here we use a significantly more sensitive version of in situ end-labelling, referred to as ISEL+, to show the distribution of dying cells within the embryonic cerebral cortex during the period of cortical neurogenesis. In addition, we show that this PCD has apoptotic characteristics by virtue of the presence of 'nucleosomal ladders' detected by blunt-end ligation mediated PCR (LMPCR). Cell death is widespread and varies quantitatively during development. Many dying cells are observed in postmitotic cortical layers where initial synaptic connections are being formed, but the majority are found within the non-synaptic regions of cell proliferation.

## MATERIALS AND METHODS

### Tissue collection and preparation

A total of 53 embryos and 17 adult Balb/c mice (Harlan-Sprague Dawley) were examined. Tissue sections were prepared as described previously (Chun et al., 1991). Briefly, timed-pregnant Balb/c female mice were killed by cervical dislocation and embryos removed rapidly, embedded in Tissue-Tek (Miles, Inc.) and quick-frozen in Histo-freeze (Fisher Scientific). Adult mice were anesthetized and killed by cervical dislocation, and the desired CNS and immune system tissues rapidly dissected and frozen for cryostat sectioning. Sections were cut at 10 μm by cryostat (Jung Frigocut 2800 E) and collected on charged slides (Superfrost Plus, Fisher Scientific). Sections were post-fixed in 4% paraformaldehyde, extracted with 0.6% Triton X-100 in 2× SSPE, and acetylated. Sections were then dehydrated through graded ethanols and, if not used immediately, stored with a desiccant at –80°C.

### Dexamethasone treatment

Young adult Balb/c mice were injected IP with 5 mg/kg dexamethasone. 8 hours later, mice were killed, and their thymuses removed and sectioned as described above.

### Retina studies

Postnatal mice at P1-P9 were anesthetized in ether, decapitated and sectioned in the horizontal plane to include retinal samples.

### In situ end-labelling plus (ISEL+)

Sections were incubated in labelling mix (100 mM potassium cacodylate, 2 mM $CoCl_2$, 0.2 mM DTT, 0.5 μM digoxigenin-11-dUTP (Boehringer-Mannheim) containing 150 U/ml terminal-deoxynucleotidal-transferase (TdT; GIBCO BRL). Sections labelled with [$^{32}$P]dCTP (DuPont NEN) were treated identically but the digoxigenin-11-dUTP was replaced with 0.02 μCi [$^{32}$P]dCTP. Slides were incubated in a humidified chamber for 1 hour at 37°C. Reactions were terminated by incubating slides in 2× SSPE at 65°C for 2 hours. Slides were then washed 3 times over 10 minutes in 1× Tris-buffered saline (TBS). Incorporated digoxigenin-11-dUTP was detected using alkaline phosphatase-conjugated anti-digoxigenin Fab fragments (Boehringer-Mannheim). Sections were incubated for 1 hour in blocking solution (1% blocking reagent (Boehringer-Mannheim) in TBS/0.3% Triton X-100), then incubated with fresh blocking solution, containing Fab fragments at a dilution of 1:500,

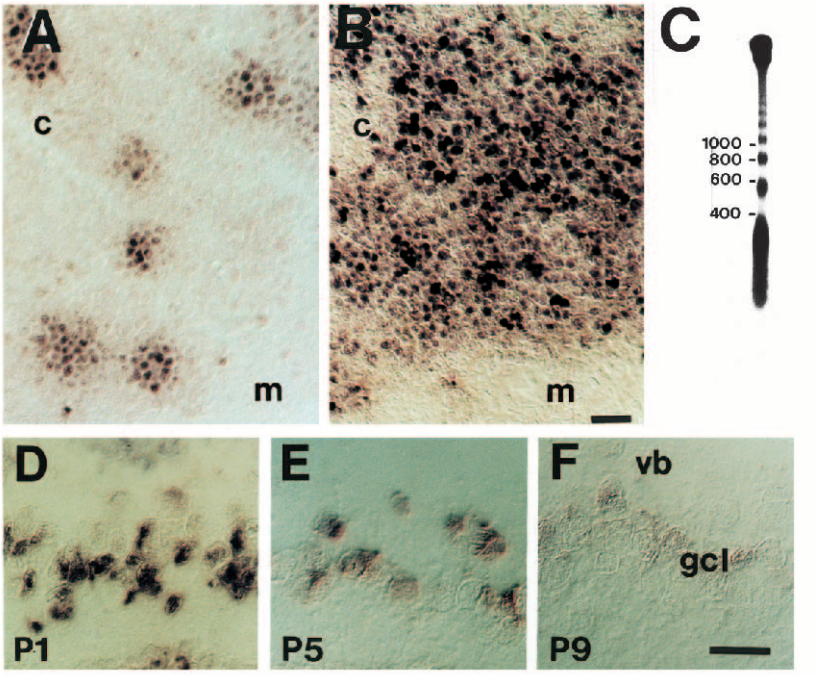


**Fig. 1**. ISEL+ identifies dying cells in tissues previously shown to undergo PCD. (A) ISEL+ labelling of a section from normal thymus reveals small clusters of dying cells within the thymic cortex. (B) ISEL+ labelling of a dexamethasone-treated thymic section. Dexamethasone induces apoptosis of CD4+/CD8+ thymocytes in the cortex (c) and not in the medulla (m). (C) Fragmented DNA isolated directly from ISEL+ labelled tissue sections of dexamethasone-treated thymus and analyzed by gel electrophoresis. Only the DNA that was labelled in situ can be visualized by this technique. The presence of characteristic nucleosomal ladders (Wyllie, 1980) demonstrates that the cells are indeed undergoing PCD (size markers in base-pairs). (D-F) ISEL+ labelling patterns in the ganglion cell layer (gcl) of the neonatal retina. The distribution of labelled cells was examined during the primary period of cell death (Young, 1984). (D) P1. Over 60% of the cells are labelled, correlating with the known peak of cell death (Lam et al., 1982; Potts et al., 1982; Perry et al., 1983; Young, 1984; Linden and Pinto, 1985; Crespo et al., 1985; Horsburgh and Sefton, 1987; Williams and Herrup, 1988). (E) P5. Cell death is decreasing at this age, with fewer than 50% of cells labelled. (F) P9. Near the end of the reported period of cell death (Young, 1984), only about 20% of cells are labelled (vb, vitreous body). The continued presence of labelled cells at P9 reflects the presence of dying, displaced amacrine cells that constitute virtually all of the dying cells in the ganglion cell layer at this age (Horsburgh and Sefton, 1987), while the reduction of dying cells during the first 2 postnatal weeks, reported here as a percentage, agrees closely with previous studies (Young, 1984; Horsburgh and Sefton, 1987). Bars, 20 μm.

overnight (12-16 hours) at room temperature. Sections were washed 3 times over 10 minutes in 1× TBS, and alkaline phosphatase activity detected by incubation in substrate solution (100 mM Tris, 100 mM NaCl, 50 mM $MgCl_2$, pH 9.5) containing 4-nitroblue tetrazolium chloride (NBT, Boehringer Mannheim) and X-Phosphate (Boehringer Mannheim). Color was allowed to develop for 2 hours, and the reaction was terminated by transferring slides into 1× TBS. After TBS washes, nuclei were stained by incubating sections in 4,6-diamino-2-phenylindole (DAPI) at a concentration of 0.35 μg/ml for 15 minutes. Sections were rinsed in Milli-Q $H_2O$, coverslips placed on top in Aquamount (Polysciences, Inc.) and cortical regions photographed.

### Histological/enzyme treatments

#### Heat-inactivated TdT

TdT was heat-denatured in Milli-Q water at 90°C for 10 minutes, cooled, then incubated as described above for ISEL+.

#### RNase treatment

Sections were incubated with 50 μg/ml DNase-free pancreatic RNase (Boehringer Mannheim) in 1× enzyme buffer for 1 hour at 37°C. Following RNase treatment, sections were washed three times over 10 minutes in 1× TBS, and end-labelled as described above.

#### DNase treatment

Sections were incubated with DNase I at a concentration of 10 μg/ml in DNase I buffer (50 mM Tris, pH 7.5, 50 μg/ml BSA) containing 10 mM $MnCl_2$ to promote double-strand cleavage of DNA. Sections were incubated at 37°C for 10 minutes, washed three times over 10 minutes in 1× TBS, and end-labelled as described.

#### Cell birthdate studies

Both bromodeoxyuridine (BrdU) and [$^3$H]thymidine were used to visualize mitotic cells in the embryonic cortex. Timed-pregnant Balb/c females were injected IP with 20 μl/g body weight of 10 mM BrdU in PBS, or 0.5 mCi [$^3$H]thymidine, at E14. After 30 minutes, females were killed by cervical dislocation and embryos were removed, fixed and sectioned as described above. Sections containing BrdU were visualized by immunohistochemistry using a mouse-anti-BrdU antibody (Boehringer Mannheim) and ABC-HRP (Vector Labs) using DAB as the chromogen. For tissue autoradiography, slides were dipped in NBT-2 emulsion (Kodak) and dried in a humidified chamber for 3.5 hours. Slides were stored in a light-tight box with desiccant at 4°C for 1 week and then developed. After developing, slides were stained with cresyl violet, dehydrated through graded ethanols and xylene, and coverslips placed on top. Slides were photographed using Nomarski optics.

### DNA isolation

Apoptotic ladders were detected in dexamethasone-treated thymuses by extracting DNA directly from ISEL+ labelled tissue sections; tissue was scraped from labelled slides with a scalpel blade, then digested in SDS-Proteinase K buffer (digestion buffer: 75 mM NaCl,

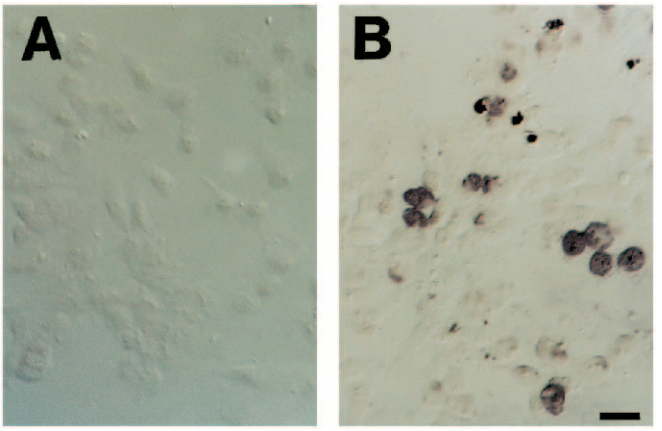


**Fig. 2.** ISEL+ identifies dying cells in a culture model of apoptosis. The ability of ISEL+ to identify cells induced to undergo apoptosis was examined following ultraviolet (UV) light induction of apoptosis in a neural cell line (Caelles et al., 1994). Undifferentiated P19 cells were grown sub-confluently on glass coverslips, then exposed to 80J/m$^2$ of UV light followed by growth for 10 hours. A control culture (A) shows rare or no labelled cells in contrast to a culture exposed to UV light (B), in which many labelled cells are observed. The labelling by ISEL+ directly correlates with the production of ladders by either end-labelling (Caelles et al., 1994) or by LMPCR (Staley, Blaschke and Chun, in preparation). Bar, 20 μm.

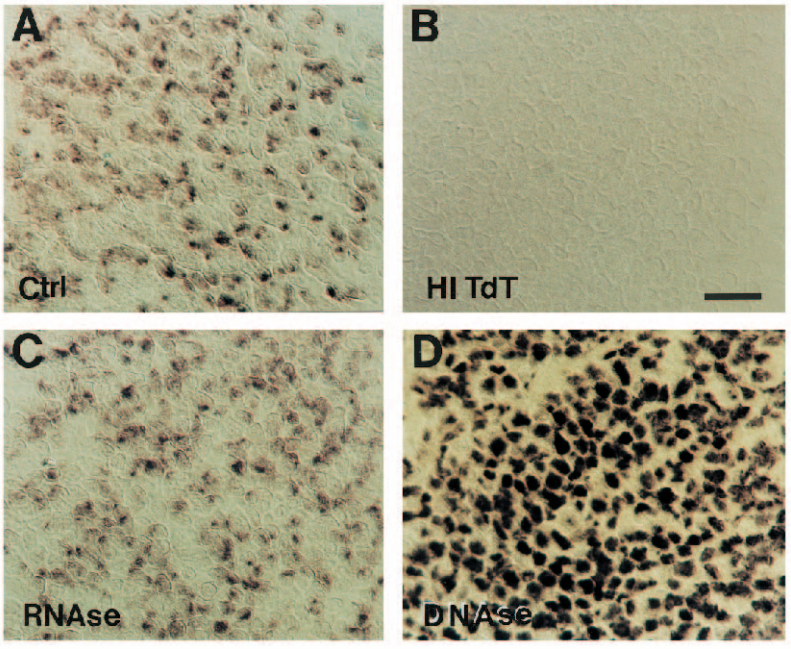


**Fig. 3.** ISEL+ is dependent on TdT activity, labels DNA but not RNA, and can access virtually all nuclei that possess available DNA ends. Consecutive sections of an E16 mouse brain were labelled in parallel after the described pre-treatment; shown for the vz. (A) control section (Ctrl), labelled as described in the Materials and Methods. (B) Heat-inactivated TdT (HITdT). The lack of labelling in any cell shows that the ISEL+ pattern is dependent on enzyme activity. (C) Pre-treatment of section with RNase. RNase digestion does not alter the labelling pattern (compare to A and to Fig. 6) showing that RNA is not detected by TdT under these conditions. (D) Pre-treatment of section with DNase. DNase pre-treatment causes double-strand DNA breaks in all cells (see Materials and Methods). After pre-treatment, all cells are labelled by ISEL+, showing that TdT can access fragmented DNA in virtually all nuclei. The observed pattern (Fig. 6) thus cannot be due to DNA inaccessibility during ISEL+ labelling. Bar, 20 μm.

25 mM EDTA, 1% w/v SDS, 10 mM Tris-HCl, pH 8, and fresh 0.4 mg/ml Proteinase K) overnight. DNA was recovered by phenol/chloroform extraction and then electrophoresed on agarose gels. DNA was transferred to a nylon membrane for anti-digoxigenin visualization (Boehringer Mannhein). For sections labelled with [$^{32}$P]dCTP, DNAs were isolated identically, then analysed on agarose gels. The hot gels were dried and exposed to film. Similar results were obtained with either labelled nucleotide, although [$^{32}$P]dCTP gave higher resolution.

DNAs were isolated for LMPCR by rapidly collecting embryonic heads in ice-cold DMEM, dissecting the cortices, then immediately lysing the cells in prewarmed digestion buffer. At ages E10-E14, 'cortices' also included other parts of the telencephalon and some mesenchymal cells that were not easily removed during the rapid dissection. After overnight digestion, DNAs were phenol/chloroform extracted, precipitated and spooled (no differences in LMPCR results were observed with pelleted DNA rather than spooled, although spooled DNA was more easily solublized after isolation). All DNAs were quantified by fluorometer.

### Cell culture for UV-induced apoptosis

The embryonal carcinoma line P19 (Rudnicki and McBurney, 1987) was grown by plating $2.5\times10^4$ cells on 12-mm coverslips in medium (Opti-MEM I (Gibco) supplemented with 5% fetal calf serum, 20 mM glucose, 55 μM β-mercaptoethanol, and penicillin-streptomycin), and incubated at 37°C for 24 hours. Before UV-irradiation, the medium was removed from experimental and control plates and the cells washed in pre-warmed PBS. After UV irradiation (80 J/m$^2$ in a GS Genelinker; BioRad), prewarmed medium was added and the plates returned to the incubator. After 10 hours, the cells were washed in PBS, fixed as described above (see Tissue collection and preparation), then processed for ISEL+.

### Blunt-end ligation mediated PCR (LMPCR)

Genomic DNA was isolated and analysed by LMPCR (Staley, Blaschke and Chun, manuscript in preparation). Briefly, 2.5 μg was mixed with 1 nmol of 24-bp and 12-bp unphosphorylated oligonucleotides, annealed and then ligated. The reactions were then diluted to a final concentration of 5 ng/μl. Samples were stored at −20°C until PCR. The sequences of blunt-end linkers used to amplify nucleosomal ladders were 24 bp: 5′-AGCACTCTCGAGCCTCTCACCGCA-3′ and 12 bp: 5′-TGCGGTGAGAGG-3′. Ligated DNA (150 ng) was used in a PCR assay containing the 24-bp linker as primer. Samples were amplified for 20 to 30 cycles of 1 minute at 94°C and 3 minutes at 72°C. PCR products were analysed by agarose gel electrophoresis, stained by ethidium bromide and photographed.

#### Control PCR for *en-2*

Identical amounts of ligated DNA (150 ng) were used in 100 μl PCR buffer (as described above, except for the presence of 4 mM $MgCl_2$), 50 μM of each dNTP, 100 pmol of each of the oligonucleotides 5′-AGGACAAGCGGCCTCGCACA-3′ and 5′-CGGTGTCC-GACTTGCC CTC-3′ and 2.5 U *Taq* polymerase. The samples were amplified for 26 cycles of PCR: 1 minute at 94°C, 1 minute at 70°C and 1 minute at 72°C. Analysis of standard amounts of DNA (50-150 ng) confirmed linear amplification of the 270-bp *en-2* fragment at this cycle number (data not shown).

### Quantitation of labelled cells

Cells were counted in photographs taken at 630×, using a Zeiss Planapo lens. Counts were taken from the ganglion cell layer of the nasal retina and from the dorsal cerebral wall of the telencelphalon. At least three different tissue sections from at least two animals were photographed at each age. For cortical cell counts, several pictures of adjacent fields were taken for each slide in each cortical area reported. All cells were counted to calculate labelled cells as a percentage of total.

## RESULTS

### ISEL+ identifies cells undergoing PCD

To optimize the sensitivity of in situ end-labelling, we examined several variables of the ISEL technique, including the choice of DNA polymerase, labelled nucleotide, visualization system and tissue preparation; the resulting technique called 'ISEL+' (see Materials and Methods) is approximately ten times more sensitive than those previously published (Blaschke, Staley and Chun, unpublished observation). To ascertain that ISEL+ identified dying cells, we examined three established models of PCD: the normal and dexamethasone-treated thymus, the postnatal ganglion cell layer of the retina, and an in vitro model of apoptosis in a neural cell line (Caelles et al., 1994).

In the normal thymus (Fig. 1A), dying cells are revealed in the thymic cortex by ISEL+, consistent with previous observations (Surh and Sprent, 1994). Exposing the thymus to dexamethasone is known to result in a massive increase in PCD amongst immature T-cells (Wyllie, 1980), and this increase is revealed by ISEL+ (Fig. 1B). Cells labelled by ISEL+ in both the normal and treated thymus were primarily found in the thymic cortex, where it has been shown that approximately 97% of young $CD4^+/CD8^+$ thymocytes die (Matsuyama et al., 1966; Egerton et al., 1990; Shortman et al., 1990; Surh and Sprent, 1994). To ascertain that the labelled DNA ends visualized in situ were derived from cells undergoing apoptosis, DNA was isolated directly from ISEL+ labelled, dexamethasone-treated thymic tissue sections, analyzed by gel electrophoresis and the labelled DNA visualized (Fig. 1C). Only those DNA fragments that had been end-labelled in situ were detected. Using this technique, the DNA fragments characteristic of apoptosis, nucleosomal ladders, were observed (Wyllie, 1980), consistent with ISEL+ identifying apoptotic cells in this model system. PCD observed previously in the adult small intestine (Gavrieli et al., 1992) and embryonic limb bud, was also identified by ISEL+ (Blaschke, Staley and Chun, unpublished observation). Thus, ISEL+ detects normal apoptosis in the thymus and other tissues, and reveals the relative increase in apoptotic cells that occurs following the induction of cell death by dexamethasone treatment of the thymus.

A CNS model for PCD is the loss of cells within the ganglion cell layer of the neonatal rodent retina (Lam et al., 1982; Potts et al., 1982; Perry et al., 1983; Young, 1984; Linden and Pinto, 1985; Crespo et al., 1985; Horsburgh and Sefton, 1987; Williams and Herrup, 1988). Within this retinal layer, as many as 66% of the ganglion cells observed at birth are eliminated by the first postnatal week (Crespo et al., 1985; Horsburgh and Sefton, 1987), while a similar magnitude of death occurs amongst displaced amacrine cells within this same layer during the second postnatal week (Horsburgh and Sefton, 1987). ISEL+ identified dying cells (Fig. 1D-F) with a relative magnitude and absolute time course that was consistent with previous reports.

In addition to tissue models, ISEL+ was used to examine the induction of apoptosis following ultraviolet (UV) light damage to neural cell lines (Caelles et al., 1994). Undifferentiated P19 cells (Rudnicki and McBurney, 1987) were grown as a monolayer on coverslips and examined by ISEL+ (Fig. 2A), which revealed rare or no labelled cells in a microscopic field.

By contrast, cultures exposed to UV light to induce apoptosis (Fig. 2B) contained many labelled cells, consistent with the documented increase in detectable apoptotic ladders (Staley, Blaschke and Chun, unpublished data; Caelles et al., 1994).

To further define ISEL+ characteristics, several control experiments were conducted on tissue sections from embryonic cortex (Fig. 3). Heat inactivation of TdT prevented labelling (Fig. 3B), while RNase pre-treatment of the section (Fig. 3C) did not produce a change compared to the control (Fig. 3A). Pre-treatment of sections with DNase under conditions that produced double-strand DNA breaks allowed ISEL+ labelling of virtually all cells (Fig. 3D). These results demonstrate that ISEL+ labels the free ends of DNA but not RNA through TdT activity, and that TdT can access fragmented DNA in virtually all nuclei.

Another potential source of free DNA ends are single-strand Okazaki fragments produced during discontinuous DNA synthesis (although the employed TdT conditions for ISEL+ favour double-strand breaks; see Materials and Methods). To examine the possible labelling of Okazaki fragments, the location of cells actively undergoing DNA synthesis in the embryonic cortex was compared to the pattern of ISEL+ labelling. Following a 30 minute pulse of BrdU or [$^3$H]thymidine (shown for BrdU) at embryonic age 14 (E14), the cells of the developing cortex undergoing DNA synthesis could be identified in situ, revealing a band of labelled cells within the vz (Fig. 4A). In contrast, ISEL+ did not reproduce an identical band of labelling in the cortex, but instead labelled cells throughout the cerebral wall (Fig. 4B). Thus, patterns of ISEL+ labelling cannot be explained by the detection of cells replicating their DNA. Based on these controls and on the ability of ISEL+ to recognize PCD in three independent model systems, ISEL+ was used to examine PCD during embryonic cortical development.

## Embryonic PCD is widespread and changes developmentally

The widespread distribution of dying cells detected by ISEL+ within the embryonic cortex is shown in Fig. 5A, as compared to DAPI staining of the same section (sagittal view at E16; Fig. 5B). The cerebral wall shows a fairly uniform distribution in the rostral-caudal dimensions, and this uniformity is at least superficially conserved in the lateral-medial dimensions (data not shown). In addition, dying cells are visible in other parts of the nervous system (Fig. 5; ganglionic eminence, g). The distribution of dying cells in the embryonic layers of the cerebral wall can be seen more clearly in the enlarged mid-dorsal views in Fig. 6. Cortices were examined during neurogenesis, embryonic days 10-18 (E10-E18), and compared to the adult cortex. Sections labelled by ISEL+ (Fig. 6A,C,E,G,I,K) are shown adjacent to DAPI staining of the same section. The majority of dying cells are observed after E12, with the apparent peak of PCD occurring around E14 (based on the percentage of cells dying; see also Fig. 9). In contrast, few dying cells are seen at E10 or in the adult cortex.

To confirm that apoptosis was occurring within the cortex at these ages, DNAs from identical ages to those shown in Fig. 6 were examined by blunt-end ligation-mediated PCR (LMPCR; Staley, Blascke and Chun, manuscript in preparation), which specifically and sensitively amplifies apoptotic DNA fragmentation (nucleosomal DNA ladders) in a semi-quantitative manner. The technique reproducibly identifies ladders in both in vitro and in vivo apoptotic model systems. As seen in Fig. 7, the relative amounts of nucleosomal ladders revealed by LMPCR directly correlated with the percentage of ISEL+ identified cells; ladders were present from E12 through E18 but were barely detectable at E10 and in adulthood. As a comparison, LMPCR of DNA from an adult thymus is also shown. These data indicate that ISEL+ indeed recognizes PCD in the cortex, as it does in other systems, and moreover, that the death is likely to occur through an apoptotic pathway.

## PCD occurs in both mitotic and postmitotic regions

Many dying cells were observed in the postmitotic regions of the cerebral wall, the cp, marginal zone (mz) and intermediate zone (iz), after their formation by E16 (Fig. 6). However, the majority of dying cells were observed within the proliferative zones: either the primordial plexiform layer (ppl; E12-E14) or the vz (E16-E18). Enlargements of the major embryonic zones at E16 are shown in Fig. 8: the postmitotic cp and iz (Fig. 8A-D), and the mitotic vz (Fig. 8E,F). Note that cells detected by ISEL+ are present in both the postmitotic and mitotic zones, and that the majority of PCD is located within the proliferative zones, the ppl and vz (see also Fig. 9). As expected, labelling was nuclear in cells of all zones, as demonstrated by the presence of label within DAPI-stained nuclei (Fig. 8B,D,F; arrows), some of which appear pyknotic (Fig. 8E,F; open arrows). Throughout the cerebral wall, most dying cells are probably of neuronal lineages, based on previous studies of cortical development (Berry and Rogers, 1965; Hicks and D'Amato, 1968; Rakic, 1977; Das, 1979; see Discussion). At the border between the subplate (sp) and cp, note the large, labelled cells (see Discussion). The identity of dying cells in the proliferative zones is less certain than in postmitotic zones, although based on their birthdates, at least some of them are likely to be of neuronal lineages (see Discussion).

## Quantitative changes in PCD through development

The quantitative distribution of dying cells revealed by ISEL+ (Fig. 6) during embryonic development is summarized in Fig. 9. Embryonic zones were photographed, all cells from each zone were counted and the labelled cells were expressed as a percentage of the total number of cells (see Materials and Methods). Three features are notable: (1) PCD varies developmentally such that at E10 and in the adult cortex, less than 1% of cortical cells are dying; (2) from E12 through E18, dying cells range from 25% to over 70%, with an average around 50% – note that despite similar percentages of labelled cells in the cp and vz, the number of labelled cells is greater in the vz since this is a region of higher cell density; and (3) the peak of cell death occurs around E14. Thus, these features indicate that very early in cortical development, at E10, PCD is virtually absent; however it subsequently increases to a peak at E14, then declines to lower but significant levels by the end of neurogenesis. PCD declines to adult levels sometime during postnatal life.

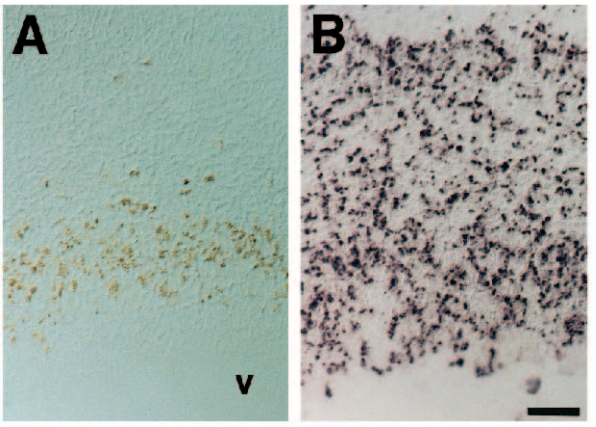


**Fig. 4.** The detection of cells synthesizing DNA cannot explain the distribution of ISEL+ labelled cells. (A) The location of cells actively undergoing DNA synthesis in the embryonic cortex at E14 was detected by a 30 minute pulse of BrdU, followed by tissue sectioning and anti-BrdU immunohistochemistry. The labelled cells appear brown. (B) The distribution of cells undergoing DNA synthesis was compared to the pattern of cells labelled by ISEL+ in an immediately adjacent section. The ISEL+ pattern is widespread, and does not reproduce the distribution of BrdU-labelled cells shown in A, although a minor degree of overlap may exist. Hence, free DNA ends associated with DNA synthesis cannot account for the labelling pattern seen with ISEL+. v, ventricle. Bar, 50 μm.

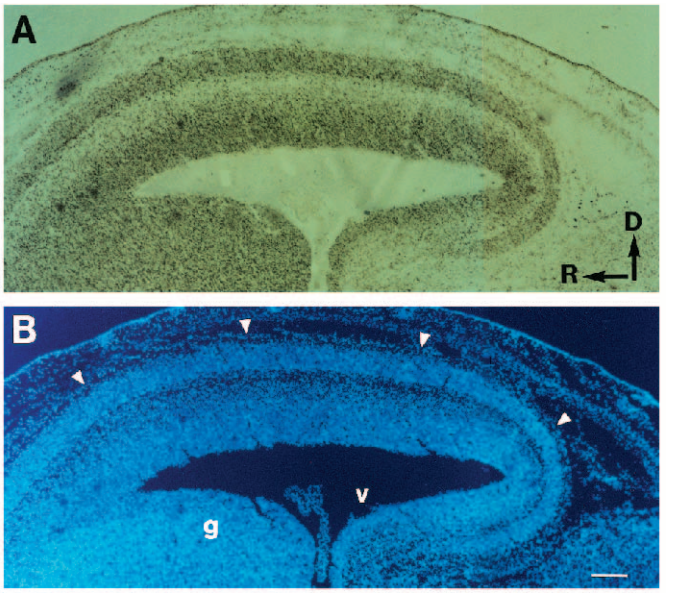


**Fig. 5.** Low magnification view of ISEL+ labelling throughout the E16 cortex. The overall distribution of dying cells in the E16 cortex, as revealed by ISEL+ (A) and compared to nuclear DAPI staining of the same field (B). (A) A low magnification saggital section through the E16 cortex reveals the widespread distribution of labelled cells within the embryonic cortex at this age. In rostral-caudal dimensions the pattern of labelling in the cortex is relatively uniform. In dorsal-ventral dimensions, however, the three embryonic layers of the developing cortex can be distinguished by their different densities of labelling (see also Figs 6G,H and 8). ISEL+ labelling is also seen throughout the developing nervous system, such as the ganglionic eminence (cf. B: g). (B) Nuclear DAPI staining of the E16 cortex shows the location of all the cells within the section. Arrowheads indicate the outer surface of the cortex, below the pia and the skull. Bar, 200 μm. D, dorsal; R, rostral; g, ganglionic eminence; v, ventricle.

## DISCUSSION

We have documented the developmental distribution of dying cells in the embryonic cerebral cortex for the period spanning neurogenesis, E10-E18, using a sensitive DNA end-labelling technique referred to as ISEL+. During this period, an average of 50% of cortical cells are undergoing PCD. Based on percentages of dying cells, it appears that widespread PCD commences after E10, reaches a peak around E14, then decreases postnatally to the low levels seen in the adult. Dying cells are observed throughout the cerebral wall, but the majority are located within proliferative zones.

Although there is no evidence for mechanisms other than PCD that biologically produce massive DNA fragmentation, end-labelling DNA in itself is not specific for PCD. Previous studies, however, have established that related forms of ISEL identify PCD specifically (Gavrieli et al., 1992; Wood et al., 1993; Wijsman et al., 1993; White et al., 1994; Homma et al., 1994), and these observations were extended here to demonstrate that ISEL+ indeed identifies dying cells in three established models of PCD (Figs 1-2). ISEL+ reveals normal apoptosis and the quantitative increase in apoptosis following dexamethasone treatment of the thymus within the expected anatomical compartment, the thymic cortex (Wyllie, 1980; Shortman et al., 1990; Egerton et al., 1990; Surh and Sprent, 1994). Furthermore, DNA labelled by ISEL+ in tissue sections of dexamethasone-treated thymus is detected as the characteristic nucleosomal ladders observed during apoptosis (Wyllie, 1980, 1981; Wyllie et al., 1984). In the retina, ISEL+ identifies dying cells within the ganglion cell layer with a time course that parallels previous studies (Young, 1984; Horsburgh and Sefton, 1987); while the percentages of dying cells at P5 and P9 may at first appear surprising, the presence of many dying displaced amacrine cells within the ganglion cell layer (Horsburgh and Sefton, 1987) explains these profiles during and after this period. Using a model culture system in which apoptosis is induced by UV light exposure, dying cells are again identified by ISEL+ as compared to pre-treatment controls.

The patterns of ISEL+ labelling cannot be explained by histological artifact (Fig. 3) nor by the detection of Okazaki fragments of discontinuous DNA synthesis (Fig. 4). Moreover, the developmental changes in cortical apoptosis were supported by independent analyses using blunt-end LMPCR to demonstrate the presence of nucleosomal ladders at ages where ISEL+ detected extensive death, and the relative absence of ladders from ages with little ISEL+ labelling. Therefore, ISEL+ appears highly sensitive in its detection of dying cells, and also specific in identifying much less PCD in the thymus and cell lines before the induction of apoptosis. Along with the controls shown, the patterns of labelled cells revealed by ISEL+ in the embryonic cortex are consistent with the operation of apoptosis on a large scale.

This substantial degree of PCD in the embryonic cortex is consistent with PCD documented in other parts of the developing nervous system. Analyses of PCD in spinal cord, periph-

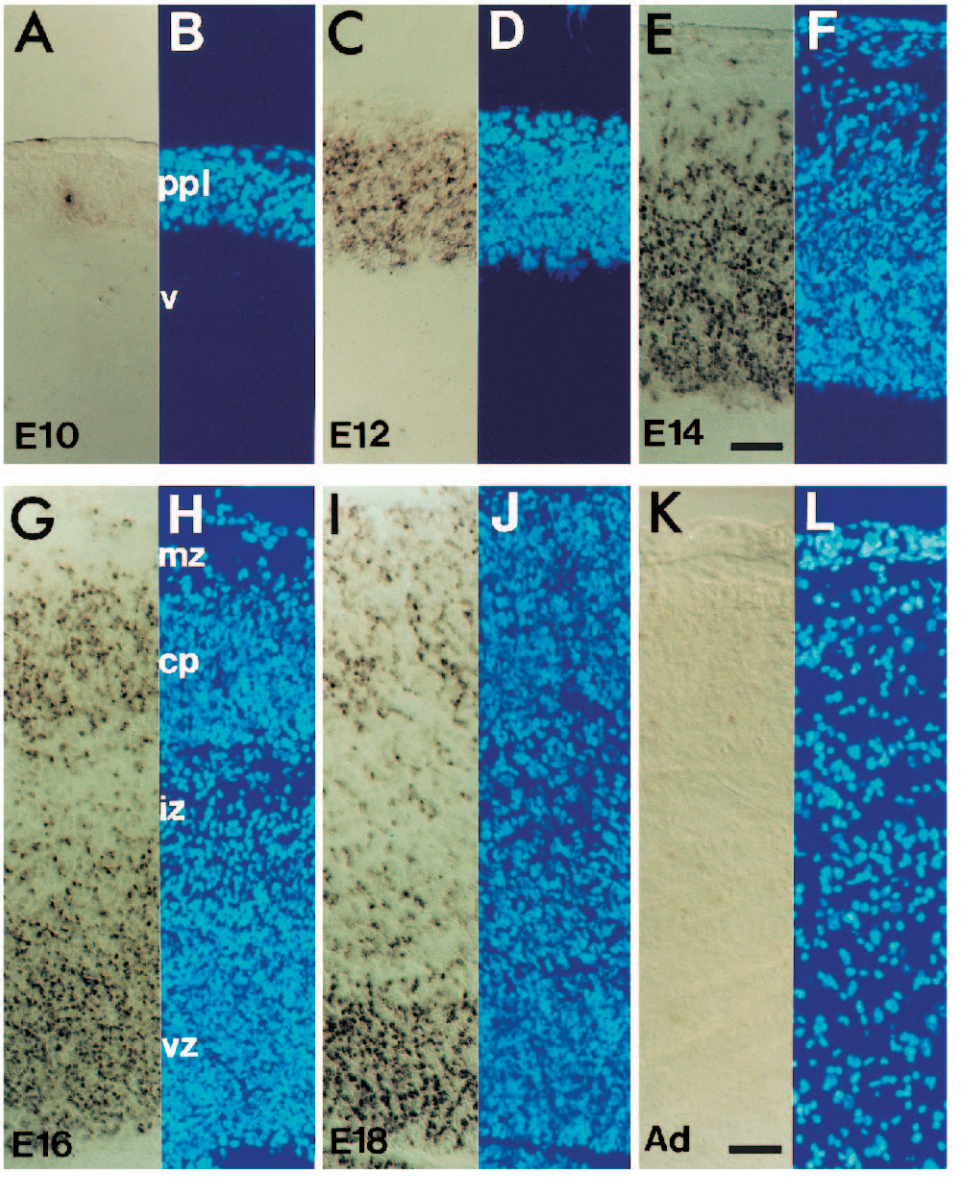


**Fig. 6**. Distribution of dying cells in the embryonic mouse cortex revealed by ISEL+ from embryonic days 10-18 (E10-E18) and the adult cortex (A,C,E,G,I,K), along with nuclear DAPI staining of the same field (B,D,F,H,J,L). (A,B) E10; from this age through E14 (A-F), the neuroepithelium consists of a homogeneous-appearing proliferative layer (B: ppl). (C,D) E12. (E,F) E14. (G,H) E16; the cerebral wall at E16 has stratified into additional layers (H: mz, cp, iz, vz) that are also apparent at E18 (I,J). (K,L) Adult cortex. The ventricle (B: v) is at the lower edge of each photograph. Note the sparse labelling at E10 that increases through E14, and then declines with further development. From E12-E18, note the extensive labelling in the proliferative zones (ppl, vz) as well as in the postmitotic zones (mz, cp, iz). Only rare dying cells are detected by ISEL+ in the adult cortex. Thus, cortical PCD is developmentally regulated and ceases by adulthood. Bars, 50 μm. ppl, primordial plexiform layer; v, ventricle; mz, marginal zone; cp, cortical plate; iz, intermediate zone; vz, ventricular zone.

eral ganglia, retina and optic nerve, where total populations of cells can be followed, indicate that PCD operates at a similar magnitude (Hamburger and Levi-Montalcini, 1949; Flanagan, 1969; Landmesser and Pilar, 1974; Hamburger, 1975; Clarke et al., 1976; Young, 1984; Crespo et al., 1985; Oppenheim, 1985, 1991; Williams and Herrup, 1988; Barres et al., 1992; Raff et al., 1993). For example, the magnitude of PCD observed here is consistent with data on the rodent retina, where 50-66% of ganglion cells die during development (Lam et al., 1982; Potts et al., 1982; Perry et al., 1983; Young, 1984; Linden and Pinto, 1985; Crespo et al., 1985; Williams and Herrup, 1988).

The rate of cell removal in the embryonic cortex cannot be determined from our data, requiring instead real-time visualization of individual dying cells. Estimates from other developing systems suggest that cell removal can occur rapidly, in hours (Flanagan, 1969; Wyllie, 1980; Barres et al., 1992; Raff et al., 1993), although we note that these estimates cannot directly address the rate of removal of cells detected by more sensitive techniques like ISEL+. Moreover, removal time appears to depend on the type of cell that is dying. Hence, in the retina, cell removal of post-mitotic ganglion cells was estimated to require up to 24 or 48 hours (Miller and Oberdorfer, 1981; Cunningham et al., 1982; Horsburgh and Sefton, 1987), even when dying cells were identified by much less sensitive morphological criteria.

The extent of cell death in the embryonic cortex that we observe raises a critical issue. If, on average, about 50% of the cells are being eliminated, then significant supernumerary cell production must occur concomitantly to replace the lost cells and to produce the observed increases in cortical cell number. Recent studies on the rate of cortical neurogenesis have provided evidence for exponential increases in cell production that could compensate for the extent of cell death observed here (Takahashi et al., 1995; Caviness et al., 1995). Interestingly, a single blast cell present at E11 is estimated to give rise to over 250 neurons (Caviness et al., 1995) and, for some

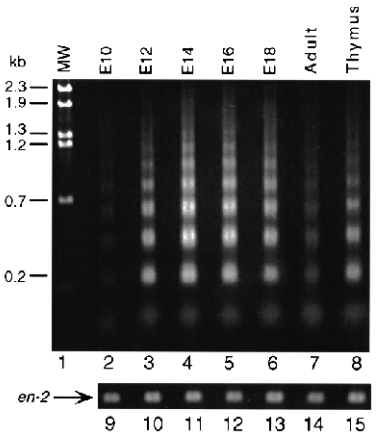


**Fig. 7.** Apoptotic DNA fragmentation (nucleosomal ladders) is detected by ligation mediated PCR (LMPCR) at the same developmental stages as PCD is identified by ISEL+ (Fig. 6). Following blunt-end linker ligation and LMPCR, PCR products were analysed by agarose gel electrophoresis and visualized by ethidium bromide staining. LMPCR detects the presence of nucleosomal ladders from E12 through E18 (lanes 3-6), but barely detects them at E10 or in the adult (lanes 2 and 7). For comparison, a DNA sample from the normal thymus analysed identically is shown (lane 8). A control PCR for the mouse *en-2* gene shows that equivalent amounts of DNA were analysed in each sample (lanes 9-15). λ-Bst E II molecular size markers are shown (lane 1).

blasts, theoretically as many as $2^{11}$ or 2048 neurons may be produced. This appears to be inconsistent with the more modest observed increase in cortical size (or small clones marked by retroviruses; see below) during the period of cortical neurogenesis, and the extent of PCD that we observe may in part explain this discrepancy.

The identity of the dying cortical cells is probably neuronal, based on previous studies showing that E10-E18 envelops cortical neurogenesis, and that glia arise around E18 or later in postnatal life (Berry and Rogers, 1965; Hicks and D'Amato, 1968; Das, 1979; Woodhams et al., 1981; Caviness, 1982; Mission et al., 1991; Takahashi et al., 1993). Some of the large labelled cells seen in Fig. 8 may be dying subplate neurons (Fig. 8C,D; curved arrows) (Shatz et al., 1988; Bayer and Altman, 1990; Kostovic and Rakic, 1990; Wood et al., 1992). This population decreases postnatally (Chun and Shatz, 1989), and our results suggest that a mechanism for their disappearance is PCD that commences before birth. It is possible that both neurons and glia are generated from pluripotent blasts, consistent with in vitro studies (Davis and Temple, 1994), but that only neurons survive during this early developmental period. Double-labelling techniques, combining ISEL+ with other markers may allow the identification of dying cells in the future.

A remarkable feature of the cortical cell death observed here is that the majority of dying cells are found within the proliferative rather than the postmitotic zones. In postmitotic regions, where neurons are forming synaptic connections (Shatz et al., 1988), target-dependent mechanisms have been described (Hamburger and Levi-Montalcini, 1949; Hamburger, 1975; Clarke et al., 1976) that could account for PCD. Classical 'matching' between neurons and their targets (Cowan et al., 1984) would be the anticipated result. Such mechanisms, however, cannot account for PCD in the proliferative zones where neurons are as yet naive to their adult targets. PCD of this nature has not been previously reported in mammals, but somewhat resembles PCD in the embryonic chick spinal cord (Homma et al., 1994). Novel mechanisms may regulate PCD in these proliferative zones.

The peak of cell death at E14 is notable, since the first neurons destined to comprise the mature cortex are being generated around this age (Caviness, 1982). Before E14, transient subplate neurons and Cajal-Retzius cells are generated (Shatz et al., 1988; Bayer and Altman, 1990; Derer and Derer, 1990). We speculate that the PCD peak around E14 may allow the selection of the first cortical neurons having desired phenotypes, which could serve as a template for the selection of later generated cells. A parallel exists between our data and PCD in the thymus where, similarly, cell death takes place in conjunction with cell proliferation (Shortman et al., 1990). Thymic PCD produces over 97% cell loss (Shortman et al., 1990) and occurs through the selection of functionally and molecularly distinct thymocytes by the surrounding stroma (Surh and Sprent, 1994). The PCD observed in the embryonic cortex may involve similar processes of cell selection.

This vast extent of PCD could be an important variable to consider in previous studies on cortical development. For example, in experiments where embryonic brains were X-irradiated, cell loss was not limited to the mitotic zones where it was expected, but was widespread and massive (Bayer and Altman, 1991). Since this form of radiation induces double-strand DNA breaks that are also generated during PCD (Wyllie, 1980, 1981; Wyllie et al., 1984), the widespread destruction of cortical cells could be explained by cells at different stages of PCD being synchronously and lethally overloaded with double-strand DNA breaks (Friedberg, 1985).

Retroviral lineage estimates of the size, distribution (Luskin et al., 1988; Walsh and Cepko, 1988; Price and Thurlow, 1988) and composition (Luskin et al., 1988; Price and Thurlow, 1988; Parnavelas et al., 1991) of cortical clones may have been underestimates. If up to 70% of cells are dying during cortical neurogenesis, then it would be likely that a given lineage could be affected by PCD, resulting in the elimination of entire clones or clone members. PCD may account for the discrepancy between the small clones of neurons or glia observed following retroviral infection in vivo (Luskin et al., 1988; Price and Thurlow, 1988) contrasting with the large, mixed clones of neurons and glia in primary culture (Davis and Temple, 1994), where disruption of normal PCD by conditions optimized for cell survival may prevent the elimination of glia or neurons from a pluripotent clone. These opposing observations could thus be explained by the previously unrecognized operation of PCD within the embryonic cortex.

The PCD documented here can now be considered in analyses of embryonic cortical development. Variability in the amount of PCD during different stages of fetal life may indicate the operation of selective mechanisms that place limits on the postnatal complement of cortical cells. While target-dependent PCD has been of primary interest in the developing nervous system, our results indicate that it is preceded by a

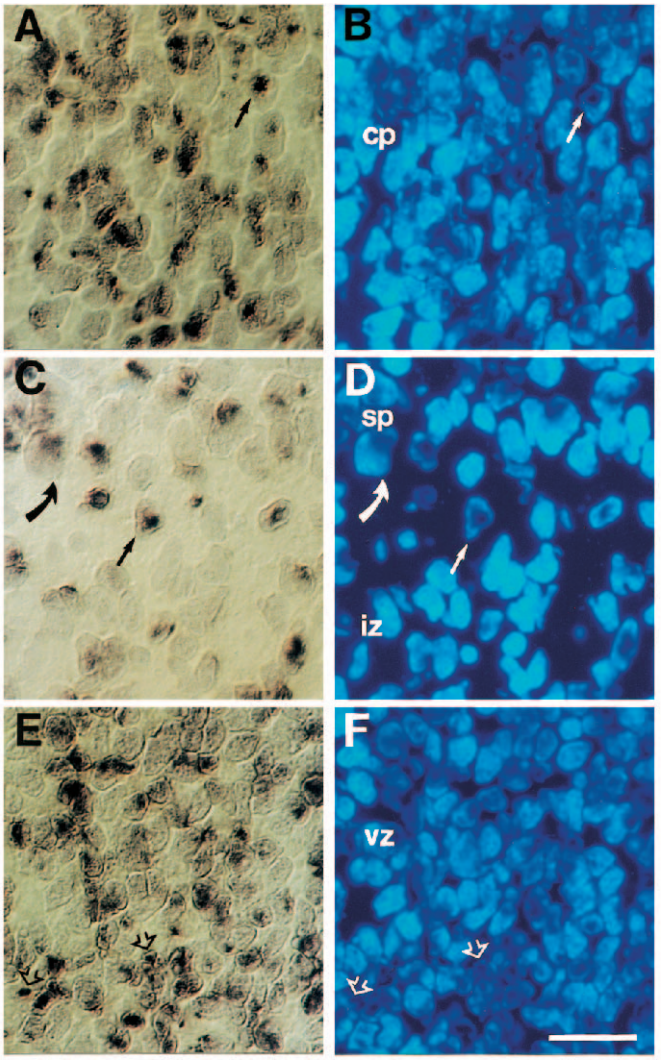


**Fig. 8**. ISEL+ produces nuclear labelling of dying cells. ISEL+ detection of dying cells (shown at E16; A,C,E) is compared to DAPI staining of the same field (B,D,F). While many cells are labelled in each area, some neighboring cells remain completely label-free, thus showing that diffusion of reaction product does not label cells. Further, the label is present within the DAPI-stained nuclei, consistent with the end-labelling of fragmented genomic DNA (A-D, straight arrows). Large, labelled cells are apparent at the cp-sp border, and are probably subplate neurons (Shatz et al., 1988) (C,D; curved arrows); similar large cells are seen in the marginal zone (not shown at high magnification, but see Fig. 6). Pyknotic nuclei are also occasionally seen (F, open arrows). Bar, 20 μm. cp, cortical plate; sp, subplate; iz, intermediate zone; vz, ventricular zone.

distinct phase of cell selection that occurs in proliferative zones, and may utilize novel regulatory mechanisms. Extensive PCD in proliferative and postmitotic zones may well be a general feature of embryonic CNS development, requiring cells to survive several phases of selection before reaching maturity.

We thank Drs D. Berg, K. Murre and D. Sretavan for reading the manuscript, and C. Akita for her expert technical assistance. This research was supported by the Esther A. and Joseph Klingenstein Fund and the California Tobacco Disease Related Program (J.C.) A.B.

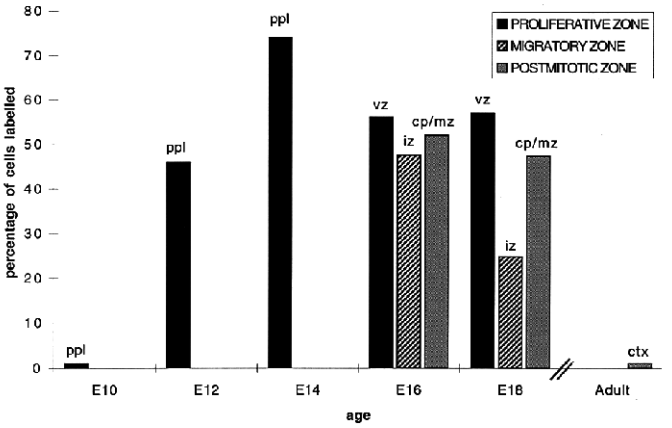


**Fig. 9**. The percentage of dying cells during embryonic development of the cerebral cortex, as detected by ISEL+. Data from the adult cortex are shown as a comparison. Labelled cells are expressed as a percentage of the total number of cells within defined regions of the cortex. The precise number of cells that are removed cannot be determined without real-time data. At E10 and in the adult, less than 1% of cells are labelled. In contrast, between E12 and E18, the percentage of labelled cells ranges from 25% to over 70%. Although the percentage of labelled cells in both the cp and vz are similar, the total number of cells present per microscopic field (24,225 $\mu m^2$) is greater in the vz. For example, at E16, cell counts averaged 396 in the cp and 496 in the vz. Thus, there are approximately 25% more cells in the vz, although we note that changes in cell size and density during this period make absolute numbers difficult to obtain. Hence, these results indicate that the majority of labelled cells are located within proliferative zones between E12-E18. ppl, primodial plexiform layer; vz, ventricular zone; iz, intermediate zone; cp, cortical plate; mz, marginal zone; ctx, cortex.

is a predoctoral fellow of the Pharmaceutical Manufacturer's Association and receives a NIH training grant.

## REFERENCES

**Abrams, J. M., White, K., Fessler, L. I. and Steller, H.** (1993). Programmed cell death during *Drosophila* embryogenesis. *Development* **117,** 29-43.

**Austin, C. P. and Cepko, C. L.** (1990). Cellular migration patterns in the developing mouse cerebral cortex. *Development* **110,** 713-732.

**Barres, B. A., Hart, I. K., Coles, H. S., Burne, J. F., Voyvodic, J. T., Richardson, W. D. and Raff, M. C.** (1992). Cell death and control of cell survival in the oligodendrocyte lineage. *Cell* **70,** 31-46.

**Bayer, S. and Altman, J.** (1990). Development of layer I and the subplate in the rat neocortex. *Exp. Neurol.* **107,** 48-62.

**Bayer, S. A. and Altman, J.** (1991). *Neocortical Development.* New York: Raven Press, Ltd.

**Berry, M. and Rogers, A. W.** (1965). The migration of neuroblasts in the developing cerebral cortex. *J. Anat.* **99,** 691-709.

**Boulder Committee** (1970). Embryonic vertebrate central nervous system: revised terminology. *Anat. Rec*. **166,** 257-261.

**Caelles, C., Helmberg, A. and Karin, M.** (1994). p53-dependent apoptosis in the absence of transcriptional activation of p53-target genes. *Nature* **370,** 220-223.

**Caviness, V. S. J.** (1982). Neocortical histogenesis in normal and reeler mice: a developmental study based upon [$^3$H]thymidine autoradiography. *Dev. Brain Res.* **4,** 293-302.

**Caviness, V. S. J., Takahashi, T. and Nowakowski, R. S.** (1995). Numbers, time and neocortical neuronogenesis: a general developmental and evolutionary model. *Trends Neurosci.* **18,** 379-383.

**Chun, J. J. M., Schatz, D. G., Oettinger, M. A., Jaenisch, R. and Baltimore, D.** (1991). The recombination activating gene-1 (RAG-1) transcript is present in the murine central nervous system. *Cell* **64,** 189-200.

**Chun, J. J. M. and Shatz, C. J.** (1989). Interstitial cells of the adult neocortical white matter are the remnant of the early generated subplate neuron population. *J. Comp. Neurol.* **282,** 555-569.

**Clarke, P. G., Rogers, L. A. and Cowan, W. M.** (1976). The time of origin and the pattern of survival of neurons in the isthmo-optic nucleus of the chick. *J. Comp. Neurol.* **167,** 125-142.

**Cowan, W. M., Fawcett, J. W., O'Leary, D. D. M. and Stanfield, B. B.** (1984). Regressive events in neurogenesis. *Science* **225,** 1258-1265.

**Crespo, D., O'Leary, D. D. M. and Cowan, W. M.** (1985). Changes in the numbers of optic nerve fibers during late prenatal and postnatal development in the albino rat. *Dev. Brain Res.* **19,** 129-134.

**Cunningham, T. J., Mohler, I. M. and Giordano, D. L.** (1982). Naturally occurring neuron death in the ganglion cell layer of the neonatal rat: morphology and evidence for regional correspondence with neuron death in superior colliculus. *Dev. Brain Res.* **2,** 203-215.

**Das, G. D.** (1979). Gliogenesis and ependymogenesis during embryonic development of the rat. An autoradiographic study. *J. Neur. Sci.* **43,** 193-204.

**Davis, A. A. and Temple, S.** (1994). A self-renewing multipotential stem cell in embryonic rat cerebral cortex. *Nature* **372,** 263-266.

**Derer, P. and Derer, M.** (1990). Cajal-Retzius cell ontogenesis and death in mouse brain visualized with horseradish peroxidase and electron mircroscopy. *Neuroscience* **36,** 839-856.

**Egerton, M., Scollay, R. and Shortman, K.** (1990). Kinetics of mature T-cell development in the thymus. *Proc. Natl Acad. Sci. USA* **87,** 2579-2582.

**Ferrer, I., Soriano, E., Del Rio, J. A., Alcantara, S. and Auladell, C.** (1992). Cell Death and Removal in the Cerebral Cortex During Development. *Prog. Neurobiol.* **39,** 1-43.

**Finlay, B. L. and Slattery, M.** (1983). Local differences in the amount of early cell death in neocortex predict adult local specializations. *Science* **219,** 1349-1351.

**Flanagan, A. E.** (1969). Differentiation and degeneration in the motor horn of the foetal mouse. *J. Morph.* **129,** 281-305.

**Friedberg, E. C.** (1985). *DNA Repair.* New York: W. H. Freeman.

**Gavrieli, Y., Sherman, Y. and Ben-Sasson, S. A.** (1992). Identification of programmed cell death in situ via specific labeling of nuclear DNA fragmentation. *J. Cell Biol.* **119,** 493-501.

**Hamburger, V.** (1975). Cell death in the development of the lateral motor column of the chick embryo. *J. Comp. Neurol.* **160,** 535-546.

**Hamburger, V. and Levi-Montalcini, R.** (1949). Proliferation, differentiation and degeneration in the spinal ganglia of the chick embryo under normal and experimental conditions. *J. Exp. Zool.* **111,** 457-502.

**Heumann, D. and Leuba, G.** (1983). Neuronal death in the development and aging of the cerebral cortex of the mouse. *Neuropath. Appl. Neurobiol.* **9,** 297-311.

**Hicks, S. P. and D'Amato, C. J.** (1968). Cell migrations to the isocortex in the rat. *Anat. Rec.* **160,** 619-634.

**Homma, S., Yaginuma, H. and Oppenheim, R. W.** (1994). Programmed cell death during the earliest stages of spinal cord development in the chick embryo: a possible means of early phenotypic selection. *J. Comp. Neurol.* **343,** 377-395.

**Horsburgh, G. M. and Sefton, A. J.** (1987). Cellular degeneration and synaptogenesis in the developing retina of the rat. *J. Comp. Neurol.* **263,** 553-566.

**Kostovic, I. and Rakic, P.** (1990). Developmental history of the transient subplate zone in the visual and somatosensory cortex of the macaque monkey and human brain. *J. Comp. Neurol.* **297,** 441-470.

**Lam, K., Sefton, A. J. and Bennett, M. R.** (1982). Loss of axons from the optic nerve of the rat during early postnatal development. *Brain Res.* **255,** 487-491.

**Landmesser, L. and Pilar, G.** (1974). Synaptic transmission and cell death during normal ganglionic development. *J. Physiol.* **241,** 737-749.

**Linden, R. and Pinto, L. H.** (1985). Developmental genetics of the retina: evidence that the pearl mutation in the mouse affects the time course of natural cell death in the ganglion cell layer. *Exp. Brain Res.* **60,** 79-86.

**Luskin, M. B., Pearlman, A. L. and Sanes, J. R.** (1988). Cell lineage in the cerebral cortex of the mouse studied in vivo and in vitro with a recombinant retrovirus. *Neuron* **1,** 635-47.

**Matsuyama, M., Wiadrowski, M. N. and Metcalf, D.** (1966). Autoradiographic analysis of lymphopoiesis and lymphocyte migration in mice bearing multiple thymus grafts. *J. Exp. Med.* **123,** 559-576.

**Miller, N. and Oberdorfer, M.** (1981). Neuronal and neuroglial responses following retinal lesions in the neonatal rats. *J. Comp. Neurol.* **202,** 493-504.

**Mission, J. P., Takahashi, T. and Caviness, V. S. J.** (1991). Ontogeny of radial and other astroglial cells in murine cerebral cortex. *Glia* **4,** 138-148.

**Oppenheim, R. W.** (1985). Naturally occurring cell death during neural development. *Trends Neurosci.* **8,** 487-493.

**Oppenheim, R. W.** (1991). Cell death during development of the nervous system. *Ann. Rev. Neurosci.* **14,** 453-501.

**Parnavelas, J. G., Barfield, J. A., Franke, E. and Luskin, M. B.** (1991). Separate progenitor cells give rise to pyramidal and nonpyramidal neurons in the rat telencephalon. *Cereb. Cort.* **1,** 463-468.

**Perry, V. H., Henderson, Z. and Linden, R.** (1983). Postnatal changes in retinal ganglion cell and optic axon populations in the pigmented rat. *J. Comp. Neurol.* **219,** 356-368.

**Potts, R. A., Dreher, B. and Bennett, M. R.** (1982). The loss of ganglion cells in the developing retina of the rat. *Brain Res.* **255,** 481-486.

**Price, D. J. and Blakemore, C.** (1985). Regressive events in the postnatal development of association projections in the visual cortex. *Nature* **316,** 721-724.

**Price, J. and Thurlow, L.** (1988). Cell lineage in the rat cerebral cortex: a study using retroviral-mediated gene transfer. *Development* **104,** 473-482.

**Raff, M. C., Barres, B. A., Burne, J. F., Coles, H. S., Ishizaki, Y. and Jacobson, M. D.** (1993). Programmed cell death and the control of cell survival: lessons from the nervous system. *Science* **262,** 695-700.

**Rakic, P.** (1976). Prenatal genesis of connections subserving ocular dominance in the rhesus monkey. *Nature* **261,** 467-471.

**Rakic, P.** (1977). Prenatal development of the visual system in rhesus monkey. *Phil. Trans. R. Soc. Lond.* **278,** 245-260.

**Rudnicki, M. and McBurney, M. W.** (1987). Cell culture methods and induction of differentiation of embryonal carcinoma cell lines. In *Teratocarcinoma and Embryonic Stem Cells: A Practical Approach* (ed. E. J. Robertson). New York: IRL Press.

**Saunders, J. W.** (1966). Death in embryonic systems. *Science* **154,** 604-612.

**Shatz, C. J., Chun, J. J. M. and Luskin, M. B.** (1988). The role of the subplate in the development of the mammalian telencephalon. NY: Plenum.

**Shatz, C. J. and Rakic, P.** (1981). The genesis of efferent connections from the visual cortex of the fetal rhesus monkey. *J. Comp. Neurol.* **196,** 287-307.

**Shortman, K., Egerton, M., Spangrude, G. J. and Scollay, R.** (1990). The generation and fate of thymocytes. *Sem. Immunol.* **2,** 3-12.

**Surh, C. D. and Sprent, J.** (1994). T-cell apoptosis detected in situ during positive and negative selection in the thymus. *Nature* **372,** 100-103.

**Takahashi, T., Nowakowski, R. S. and Caviness, V. S.** (1993). Cell cycle parameters and patterns of nuclear movement in the neocortical proliferative zone of the fetal mouse. *J. Neurosci.* **13,** 820-833.

**Takahashi, T., Nowakowski, R. S. and Caviness, V. S.** (1995). The cell cycle of the pseudostratified ventricular epithelium of the embryonic murine cerebral wall. *J. Neurosci.* **15,** 6046-6057.

**Walsh, C. and Cepko, C. L.** (1988). Clonally related cortical cells show several migration patterns. *Science* **241,** 1342-1345.

**White, K., Grether, M. E., Abrams, J. M., Young, L., Farrell, K. and Steller, H.** (1994). Genetic control of programmed cell death in *Drosophila*. *Science* **264,** 677-683.

**Wijsman, J. H., Jonker, R. R., Keijzer, R., van de Velde, C. J., Cornelisse, C. J. and van Dierendonck, J. H.** (1993). A new method to detect apoptosis in paraffin sections: in situ end-labeling of fragmented DNA. *J. Histochem. Cytochem.* **41,** 7-12.

**Williams, G. T. and Smith, C. A.** (1993). Molecular regulation of apoptosis: genetic controls on cell death. *Cell* **74,** 777-779.

**Williams, R. W. and Herrup, K.** (1988). The control of neuron number. *Ann. Rev. Neurosci.* **11,** 423-453.

**Wood, J. G., Martin, S. and Price, D. J.** (1992). Evidence that the earliest generated cells of the murine cerebral cortex form a transient population in the subplate and marginal zone. *Brain Res.* **66,** 137-140.

**Wood, K. A., Dipasquale, B. and Youle, R. J.** (1993). In situ labeling of granule cells for apoptosis-associated DNA fragmentation reveals different mechanisms of cell loss in developing cerebellum. *Neuron* **11,** 621-632.

**Woodhams, P. L., Basco, E., Hajos, F., Csillag, A. and Balazs, R.** (1981). Radial glia in the developing mouse cerebral cortex and hippocampus. *Anat. Embryol.* **163,** 331-343.

**Wyllie, A. H.** (1980). Glucocorticoid-induced thymocyte apoptosis is associated with endogenous endonuclease activation. *Nature* **284,** 555-556.

**Wyllie, A. H.** (1981). Cell death: a new classification separating apoptosis from necrosis. In *Cell Death in Biology and Pathology* (ed. I. D. Bowen and R. A. Lockshin), pp. 9-94. New York: Chapman & Hall.

**Wyllie, A. H., Morris, R. G., Smith, A. L. and Dunlop, D.** (1984). Chromatin cleavage in apoptosis: association with condensed chromatin morphology and dependence on macromolecular synthesis. *J. Pathol.* **142,** 67-77.

**Young, R. W.** (1984). Cell death during differentiation of the retina in the mouse. *J. Comp. Neurol.* **229,** 362-373.

(Accepted 12 January 1996)